A Computational Model of the Sympathetic Neuron for Drug Treatment Investigation in Sympathetic Hyperactivity

Finbar Argus[1], Chenchen Zhang[2], Harvey Davis[4], Ni Li[2], Jakub Tomek[2], Zhinuo Jenny Wang[3], Gonzalo Maso Talou[1], Dan Li[2], Blanca Rodriguez[3], Filipa C Simoes[5], David J Paterson[2]

[1] Auckland Bioengineering Institute, University of Auckland, New Zealand
[2] Department of Physiology, Anatomy and Genetics, University of Oxford, UK
[3] Department of Computer Science, University of Oxford, UK
[4] Department of Neuroscience, Physiology and Pharmacology, University College London, UK
[5] Institute of Developmental and Regenerative Medicine, University of Oxford, UK

Abstract

Diseases associated with sympathetic hyperactivity need improved treatments that target and account for the sympathetic nervous system. We have developed a computational model of the postganglionic sympathetic neuron (SN) that can simulate drug effects that reduce sympathetic hyperactivity, allowing high-efficiency analysis of potential drug treatments that can be further investigated experimentally. This computational model was calibrated to patch-clamp data from the spontaneous hypertensive rat (SHR).

We validated the simulated response to changes in input current, and M-type potassium channel up-regulation to demonstrate the accurate response to drug effects. We accurately predicted firing frequency, and membrane potential features for all experiments. The model can now be used for investigating drug effects and - once it has been coupled with cardiac electrophysiology (EP) models - will improve cardiac in silico trials to account for sympathetic activity.

The model predicts norepinephrine (NE) release at the neuro-cardiac junction, making it suitable to be coupled to cardiomyocyte models for predicting cardiac EP response to treatments of dysautonomia in rare diseases such as Catecholaminergic Polymorphic Ventricular Tachycardia (CPVT).

1. Introduction

Sympathetic hyperactivity occurs in diseases such as CPVT, which has a poor prognosis, with approximately 40% of patients dying within 10 years of diagnosis. Currently, a common treatment for CPVT are beta-blockers. However, they can be ineffective during high sympathetic activity (e.g. exercise), when delayed after depolarizations and sudden cardiac death can occur [1]. Therefore, improved treatments that target and account for the sympathetic nervous system are required.

Research on rare diseases, such as CPVT, often has insufficient capital investment required to screen new drugs for treatment improvements. Computational modelling and *in silico* trials are a path forward that could significantly reduce costs and times for developing new drugs, by accurately predicting effects prior to clinical trials. The current research on computational approaches for testing drug response, assessing arrhythmia risk, and performing cardiac *in silico* trials [2] fail to account for sympathetic innervation, meaning that accurate drug predictions can not yet be implemented for pathologies associated with dysautonomia. Therefore, an accurate model of the SN and neuro-cardiac junction is required to make computational cardiac EP predictions applicable. Belluzi et al. [3] developed a model of the SN with three K^+ channels, one Na^+ channel, and one Ca^{2+} channel. Tao et al. morphed this model into a sympathetic varicosity model to calculate NE release for coupling with a sino-atrial node cell [4]. However, they focused mostly on the coupling and the sino-atrial node model, without improving the SN model. We have developed a more physiologically accurate model of the postganglionic SN that includes soma, axon, varicosity, and endoplasmic reticulum, as well as Na^+, K^+, and Ca^+ dynamics handling and validated it for M-type channel upregulation prediction with patch-clamp data.

2. Methods

2.1. Computational Model

A SN model was developed with multiple compartments: soma, axon, varicosity, endoplasmic reticulum, and local intracellular regions for Ca^{2+}, as in Figure 1.

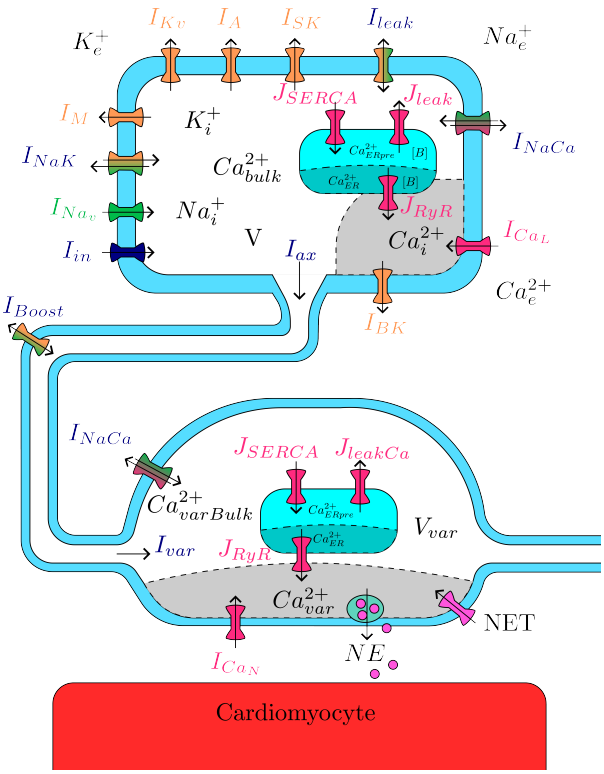

Figure 1. Sympathetic neuron schematic. I_{BK}, big calcium dependant K^+ current; I_{Ca_L}, L type Ca^{2+} current; I_{NaCa}, Na^+-Ca^{2+} exchanger; I_{leak} background Na^+ and K^+ currents; I_{SK}, slow calcium dependant K^+ current; I_A, fast K^+ current; I_M, M-type K^+ current; I_{NaK}, Na^+-K^+ pump; I_{Na_V}, total Na^+ current; I_{in}, input stimulus current; I_{ax}, axon inlet current; I_{boost}, axon membrane current; I_{var}, varicosity inlet current; I_{Ca_N}, N-type Ca^{2+} current; J_{SERCA}, SERCA pump flux; J_{leak}, endoplasmic reticulum leak flux; J_{RyR}, ryanodine receptor flux; NE, norepinephrine concentration; NET, norepinephrine transporter; $_i$ subscript, near-membrane intracellular concentration; $_e$ subscript, extracellular concentration, $_{bulk}$ subscript, bulk intracellular concentration.

All ion channels were designed in the following Hodgkin-Huxley form to allow interpretable calibration from experimental data.

$$I_i = g_i m_i h_i (V - E_i) \tag{1}$$

$$\frac{m_i}{dt} = \frac{m_i^\infty - m_i}{\tau_{i,m}} \tag{2}$$

$$m_i^\infty = \frac{1}{1 + e^{-(V+V_{i,m,50})}} \tag{3}$$

$$\tau_{i,m} = \tau_{i,m}^{min} + \frac{\tau_{i,m}^{max} - \tau_{i,m}^{min}}{e^{(V+V_{i,m,50}+V_{i,m,a})} + e^{-(V+V_{i,m,50}+V_{i,m,b})}} \tag{4}$$

$$\frac{h_i}{dt} = \frac{h_i^\infty - h_i}{\tau_{i,h}} \tag{5}$$

$$h_i^\infty = \frac{1}{1 + e^{(V+V_{i,h,50})}} \tag{6}$$

$$\tau_{i,h} = \tau_{i,h}^{min} + \frac{\tau_{i,h}^{max} - \tau_{i,h}^{min}}{e^{(V+V_{i,h,50}+V_{i,h,a})} + e^{-(V+V_{i,h,50}+V_{i,h,b})}} \tag{7}$$

where I_i is the i'th current, i relates to the I_{Na_V}, I_{Ca_N}, I_{Kv} (no h inactivation gate), I_A, I_M (no h inactivation gate) currents, g_i is the channel conductance, m_i is the activation gate coefficient, h_i is the closing gate coefficient, $\tau_{i,m}$ (the following descriptions are also the same for h) is the m gate coefficient time constant, the min and max superscripts denote the constant min and max values of that parameter, $V_{i,m,50}$ is the voltage at which $m_i^\infty = 0.5$, and $V_{i,m,a/b}$ shift the hill curve relative to $V_{i,m,50}$, to make it easier for parameter identification of $V_{i,m,50}$. In addition to these currents, we include others represented in Figure 1. The NaCa exchanger, NaK pump, and endoplasmic reticulum calcium handling were adapted from cardiomyocyte models to better represent SN Ca^{2+} concentrations. The L-type calcium channel was adapted from [3]. The full model, with all equations detailed and CellML code attached, will be published and uploaded to the Physiome Model Repository at the end of 2024.

2.2. Experimental Data

Experimental patch clamp experiments were done on excised stellate ganglia postganglionic SNs from SHRs, as detailed in [5]. Animal use was in accordance with the University of Oxford Local Ethical Guidelines, the Guide for the Care and Use of Laboratory Animals published by the US National Institutes of Health (Publication No. 85-23, revised 2011) and the Animals (Scientific Procedures) Act 1986 (United Kingdom). Experiments were performed under British Home Office Project License (PPL 30/3131 [D.J.P.] and P707EB251 [D.J.P.]).

2.3. Model Calibration and Validation

The single cell calibration and validation were done with two data sets, one baseline used for calibration and one with Retigabine application to validate the model and its predicted response to M-type potassium channel upregulation. To simulate Retigabine effects we increased the maximum M-type channel conductance (g_i) by 2.5 times (calculated by matching changes in pre-stimulation resting membrane potential), however, future work will more realistically modify the maximum conductance and shift the sigmoid curve by changing $V_{i,m/h,50}$, which is straightforward in this new formulation.

2.4. Numerical Experiments

After calibrating and validating the models we conducted numerical experiments with the model to investigate potential treatment options for reducing sympathetic hyperactivity. These numerical experiments were performed to guide future lab experiments. We investigated the response to I_{SK} up-regulation (2.5 $\times$ conductance increase) and I_{Na} block (2.5 $\times$ conductance decrease). These experiments were designed to compare against the predicted response of M-type channel upregulation and to guide future research on channel targets that might be beneficial for patients with dysautonomia.

3. Results

3.1. Model Calibration and Validation Results

The SHR model was accurately calibrated to the patch-clamp data (see Figure 2 and Table 1), with stimulation currents of 12, 44, 86, and 144 pA. Additionally, the model predicts Retigabine's (applied by increasing m-type potassium channel conductivity) effect on frequency, and max and min voltages. We successfully predict that M-type channel upregulation decreases firing rate, and shifts hyperactive SNs from tonic to phasic firing.

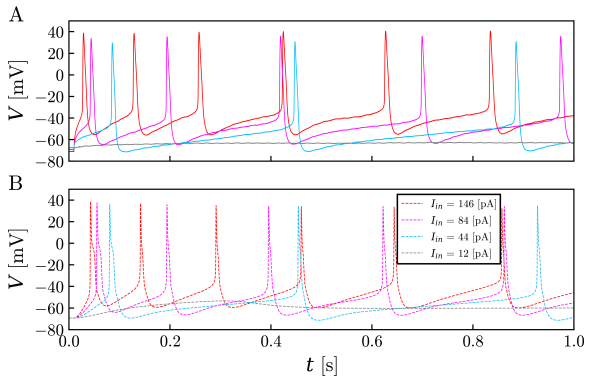

Figure 2. Baseline membrane voltage for varied stimulation current (I_{in}), showing tonic firing for (A), experimental patch clamp used for calibration, and (B), computational model predictions.

3.2. Numerical Experiment Results

Figure 4 shows calibrated SHR model response to Na channel partial block. This, compared to baseline, (Figure 2) shows change from tonic to phasic firing, however there are potentially undesired high frequency low amplitude spikes following stimulation.

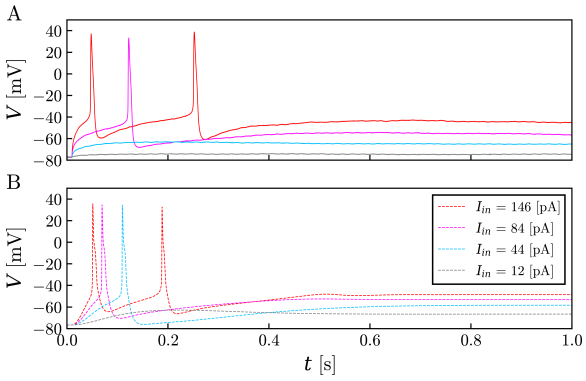

Figure 3. Response to upregulated M-type K^+ current. Membrane voltage for varied stimulation current (I_{in}), showing phasic firing for (A), experimental patch clamp used for validation (unknown in model parameter optimisation scheme), and (B), computational model predictions.

Table 1. Percentage errors for calibration (Baseline) and Validation (M-type). V_{max}, maximum voltage; V_{min}, minimum voltage; f, frequency; T_{min}, minimum period.

	V_{max} %	V_{min} %	f %	T_{min} %
Baseline 12pA	-14.3	-5.4	0.0	0.0
Baseline 44pA	17.7	1.2	0.0	3.3
Baseline 84pA	3.4	4.9	0.0	-7.9
Baseline 146pA	-5.4	8.9	0.0	-1.2
M-type 12pA	-14.8	-11.3	0.0	0.0
M-type 44pA	-154.4	-6.1	100.0	0.0
M-type 84pA	3.8	-7.0	0.0	0.0
M-type 146pA	-8.1	8.5	0.0	-32.8

Comparing Figure 5 to baseline (Figure 2) shows that upregulating I_{SK} decreases frequency from hyperactive baseline and can change tonic firing to phasic firing, such as in the 44 [pA] case.

In addition to predicting treatment response, we also predicted NE concentration in the neuro-muscular junction. Figure 6 compares NE between baseline and M-type up-regulation, showing a decrease in NE by approximately 50% after M-type channel upregulation.

4. Discussion and Conclusions

We have developed a postganglionic SN model calibrated to patch-clamp data from the SHR that can accurately predict the response to M-type K^+ upregulation (Figure 2 to Figure 3).

Cardiac computational models used for treatment response prediction need to account for the sympathetic nervous system if they are to be used for diseases that are

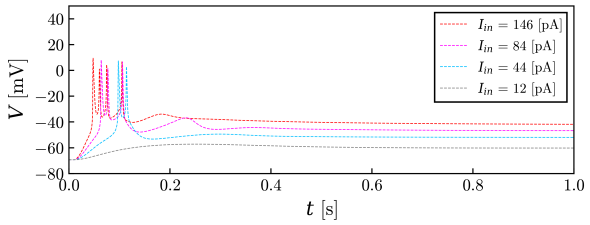

Figure 4. Voltage prediction after I_{Na} block.

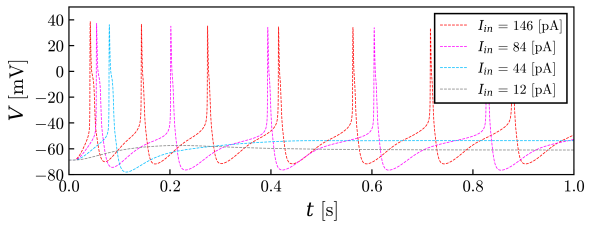

Figure 5. Voltage prediction after I_{SK} upregulation.

associated with dysautonomia, such as CPVT. Our new SN model will be able to extend cardiac EP models, and system models of cardiac control [6], so that they can accurately predict drug effects on the heart and the sympathetic control of the heart. For example, both I_{SK} modifications and I_{Na} block have been investigated in cardiac *in silico* trials. In Figures 4 and 5 we show that these drugs have significant and varied effects on the SNs that control the heart. Therefore, our model (through NE dynamics as shown in Figure 6) can provide utility by coupling to cardiac EP models for *in silico* trials that need to take into account autonomic modulation.

We have validated the model with data for M-type K^+ upregulation in the SHR, however, further validation is needed and currently being done for different drug types and in iPSC cells of CPVT patients, which may be a more effective model for CPVT patients [7]. One limitation of our approach is that we calibrate one model with parameters that may not be identifiable. However, we have developed the model to be easily calibrated, with parameters such as $V_{i,m/h,50}$ that can be modified to give physiologically realistic variability. Therefore, this model will be extendable to calibrating populations of models that replicate experimental variability to provide prediction uncertainties that give more reliable evaluation of drug risk.

Acknowledgments

We thank the Andrew Bagnall Fellowship, UGENT - VITAL (European Commission FP6), 12 Labours (MBIE), MBIE Soul Machines, the BHF (SP/F/22/150027) and the Leducq foundation (24CVD).

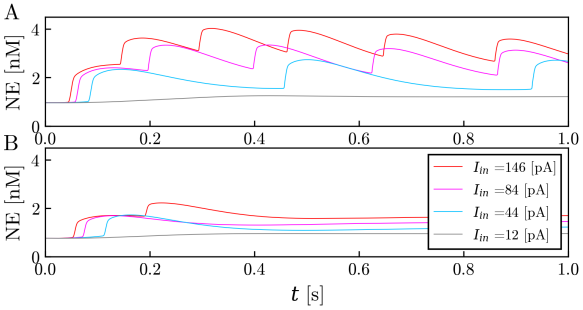

Figure 6. Predicted NE in the neuro-cardiac junction in (A) baseline and (B) after M-type channel upregulation.

References

[1] Leren IS, Saberniak J, Majid E, Haland TF, Edvardsen T, Haugaa KH. Nadolol decreases the incidence and severity of ventricular arrhythmias during exercise stress testing compared with $B1$-selective β-blockers in patients with catecholaminergic polymorphic ventricular tachycardia. Heart Rhythm February 2016;13(2):433–440. ISSN 1547-5271.

[2] Margara F, Wang ZJ, Levrero-Florencio F, Santiago A, Vázquez M, Bueno-Orovio A, Rodriguez B. In-silico human electro-mechanical ventricular modelling and simulation for drug-induced pro-arrhythmia and inotropic risk assessment. Progress in Biophysics and Molecular Biology January 2021; 159:58–74. ISSN 0079-6107.

[3] Belluzzi O, Sacchi O. A five-conductance model of the action potential in the rat sympathetic neurone. Progress in Biophysics and Molecular Biology January 1991;55(1):1–30. ISSN 0079-6107.

[4] Tao T, Paterson DJ, Smith NP. A model of cellular cardiac-neural coupling that captures the sympathetic control of sinoatrial node excitability in normotensive and hypertensive rats. Biophysical Journal August 2011;101(3):594–602. ISSN 00063495.

[5] Davis H, Herring N, Paterson DJ. Downregulation of M current is coupled to membrane excitability in sympathetic neurons before the onset of hypertension. Hypertension 2020; 76(6):1915–1923. ISSN 0194-911X, 1524-4563.

[6] Yang PC, Rose A, DeMarco KR, Dawson JRD, Han Y, Jeng MT, Harvey RD, Santana LF, Ripplinger CM, Vorobyov I, Lewis TJ, Clancy CE. A multiscale predictive digital twin for neurocardiac modulation. The Journal of Physiology 2023; 601(17):3789–3812. ISSN 1469-7793.

[7] Habecker BA, Bers DM, Birren SJ, Chang R, Herring N, Kay MW, Li D, Mendelowitz D, Mongillo M, Montgomery JM, Ripplinger CM, Tampakakis E, Winbo A, Zaglia T, Zeltner N, Paterson DJ. Molecular and cellular neurocardiology in heart disease. The Journal of Physiology 2024;ISSN 1469-7793.

Address for correspondence:

Finbar Argus, finbar.argus@auckland.ac.nz
The ABI, 70 Symonds Street, Auckland, New Zealand